

Outline of optical design and viewing geometry for divertor Thomson scattering on MAST upgrade

This content has been downloaded from IOPscience. Please scroll down to see the full text.

2013 JINST 8 C11010

(<http://iopscience.iop.org/1748-0221/8/11/C11010>)

View [the table of contents for this issue](#), or go to the [journal homepage](#) for more

Download details:

IP Address: 194.81.223.66

This content was downloaded on 20/11/2013 at 14:25

Please note that [terms and conditions apply](#).

16th INTERNATIONAL SYMPOSIUM ON LASER-AIDED PLASMA DIAGNOSTICS,
22–26 SEPTEMBER 2013,
MADISON, WISCONSIN, U.S.A.

Outline of optical design and viewing geometry for divertor Thomson scattering on MAST upgrade

J. Hawke,^{a,1} R. Scannell,^b J. Harrison,^b R. Huxford^c and P. Bohm^d

^aFOM Institute DIFFER — Dutch Institute for Fundamental Energy Research,
Association EURATOM-FOM, 3430 BE Nieuwegein, Netherlands

^bEURATOM/CCFE Fusion Association, Culham Science Centre,
Abingdon, Oxfordshire, OX14 3DB, United Kingdom

^cRBH Optics,
Burgess Hill, West Sussex RH15 8HL, United Kingdom

^dInstitute of Plasma Physics AS CR, v.v.i.,
Za Slovankou 3, 182 00 Prague 8, Czech Republic

E-mail: J.N.Hawke@diffier.nl

ABSTRACT: The super-X divertor on MAST Upgrade will be diagnosed by a Thomson scattering diagnostic. A preliminary design of the collection optics and calculations of the diagnostic's performance are discussed in this paper. As part of the design the location and size of the collection cell were optimized to minimize vignetting, especially in the region of interest close to the divertor strike point. The design process was complicated by the limited access available in the closed divertor geometry. In the study of the diagnostic's performance, the radial resolution, projection of the laser image onto the fiber bundle, and impact of depth of field with a multiple laser system were investigated. In this design there is a trade-off between the resolution of the system and the lifetime of the beam dump. For this reason the beam has its focal point at the start of the viewing region and diverges in width to approximately five millimeters near the divertor tile. The effect of this large variation in beam width is examined primarily at the two extremes by means of ray trace modeling. This model takes an object with dimensions of the beam width imaged onto the fiber bundle to investigate the effect of misalignment for a narrow or broad laser image. In a similar manner ray tracing was performed to determine the effects of depth of field for four and two laser systems. As the electron density of the system may be low, performance analysis considers firing multiple lasers simultaneously to improve photon statistics.

KEYWORDS: Plasma diagnostics - interferometry, spectroscopy and imaging; Optics; Plasma diagnostics - charged-particle spectroscopy

¹Corresponding author.

Contents

1	Introduction	1
2	Collection cell & vignetting minimization	2
3	Radial resolution	4
4	Expected fractional T_e error	5
5	Laser imaging onto fiber bundle	6
6	Depth of field for a multi-laser system	8
7	Conclusions	10

1 Introduction

Advanced divertor concepts such as a Snow-Flake divertor or Super-X divertor (SXD) are considered as possible alternatives to conventional divertors. These divertor concepts are attractive as a method to more reliably handle the high divertor power loads expected in future fusion devices [1, 2]. In an SXD, a reduction of plasma temperature and energy fluxes in the divertor is achieved by magnetic flux expansion, induced by extending the divertor leg to a larger radius and a reduction of the poloidal magnetic field within the divertor. Also, the longer connection length L_{\parallel} and closed design of the SXD supports the removal of power due to plasma-neutral interaction and radiation [3]. The introduction of a SXD configuration as part of the upcoming upgrades on the MAST spherical tokamak required the development of a diagnostic system to diagnose the plasma within this new divertor configuration. This will partly be accomplished by Thomson Scattering (TS) [4]. Figure 1 shows the design of this TS diagnostic for MAST-Upgrade.

Using Thomson Scattering to diagnose the plasma inside the SXD on MAST Upgrade allows for measurements of the electron temperature and density evolution along the extended divertor leg. This is useful in understanding the performance as well as the physics of this advanced divertor concept. Once the plasma reaches the strike point, there is expected to be a high density / low temperature detachment region which extends a few centimeters from the divertor strike point. The TS diagnostic is designed to have the capability to measure profiles of the electron temperature (T_e) and density (n_e) along the divertor leg, while also allowing for measurements of the detachment front evolution. Numerical modeling using SOL transport codes show that the T_e within the SXD on MAST-U will not exceed 100 eV, while in the detachment region near the divertor tile T_e is expected to be in the sub eV range [6]. Electron density is expected to vary from approximately $3 \times 10^{18} \text{ m}^{-3}$ to $> 10^{20} \text{ m}^{-3}$ in the detachment region. The TS diagnostic is designed to measure electron temperatures from $\sim 1 \text{ eV}$ to 100 eV and over this density range.

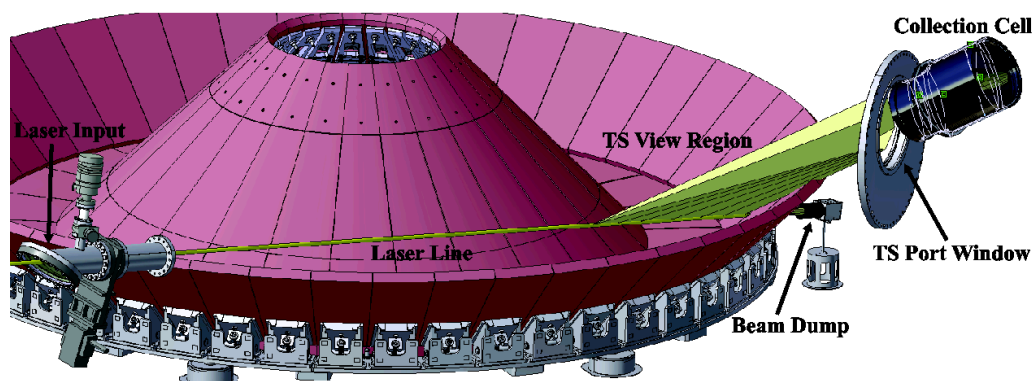


Figure 1. The MAST-U SXD TS design showing the laser injection, collection lens design, viewing region of the diagnostic, beam dump, and the divertor geometry.

In figure 2 the view region of the TS collection optics is highlighted. It is clear from this figure containing a sample super-X divertor scenario equilibrium, the laser line is not following along one field line but rather spanning over several along its path. The layout of the TS system with respect to the magnetic field lines and the effects of divertor detachment define the spatial resolution required by the system in both the radial and z directions. Although many of the parameters of the MAST-U SXD plasma are unknown, modeling using the SOL transport codes SOLPS/EIRENE along with experimental observations made on MAST provide good estimates of the diagnostic's resolution requirements [6]. In the radial direction, which extends primarily along the field lines, the resolution requirement is driven by the need to resolve the detachment front and filament structures which are both on the order of 1 cm. In the z direction which primarily spans across field lines a resolution of ~ 1 cm is required in order to capture the change in electron temperature.

2 Collection cell & vignetting minimization

The MAST Upgrade Super-X divertor presented a variety of challenges in the design of the divertor TS collection cell due to the limited access of the closed divertor geometry. The design of the collection cell required the losses due to vignetting to be minimized over the collection region. It was especially important to ensure the ability to measure the plasma effectively close to the divertor tile was preserved, in order to diagnose up to the detachment front of the diverted plasma. In order to reduce the vignetting, the vertical height and tilt of the collection lens was altered and at each orientation the vignetting losses were determined. The lens was placed as high as possible within the available port in order to minimize the vignetting close to the divertor tile. In this paper there are references to the T5 tile. This is the designation for the divertor tile which the Thomson scattering view region approaches.

In figure 3 it is clear that there are losses due to vignetting and that the size, position, and tilt of the collection optics define the resulting vignettted losses. Beyond adjusting the position and tilt of the lens, size was also considered and lenses examined spanned diameters from 150 to 200 mm. In this analysis an optimal collection cell position and orientation was determined by examining the vignetting losses along the viewing region of the laser line, shown in red in figure 3. This resulted with a 185 mm collection cell which is orientated such that the vignetting losses were specifically

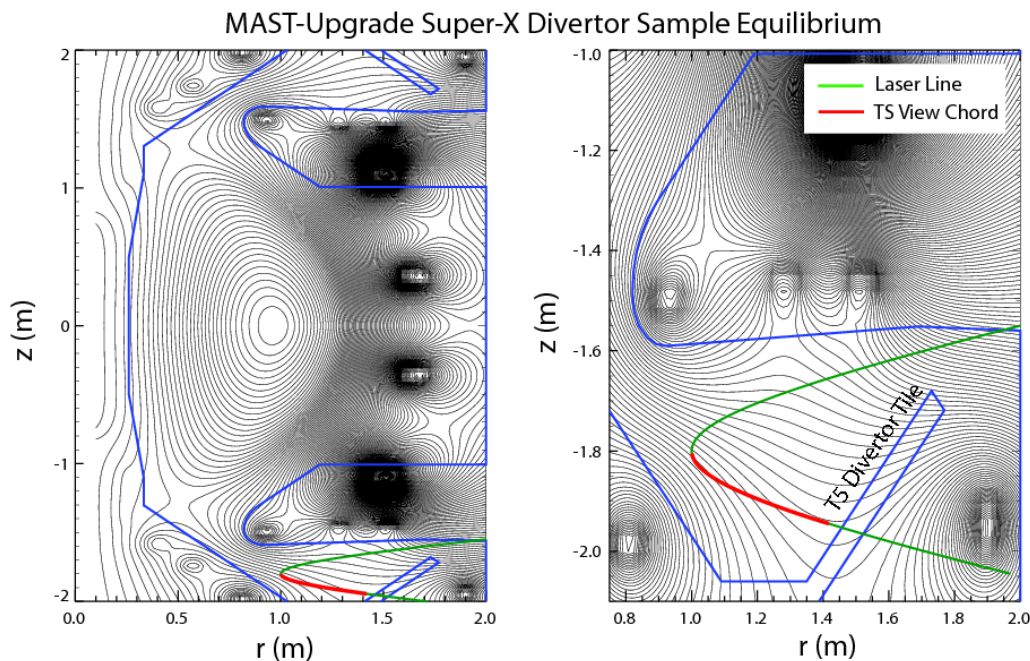


Figure 2. Shows the magnetic equilibrium of a sample super-X divertor scenario for MAST-Upgrade Tokamak in (r,z) .

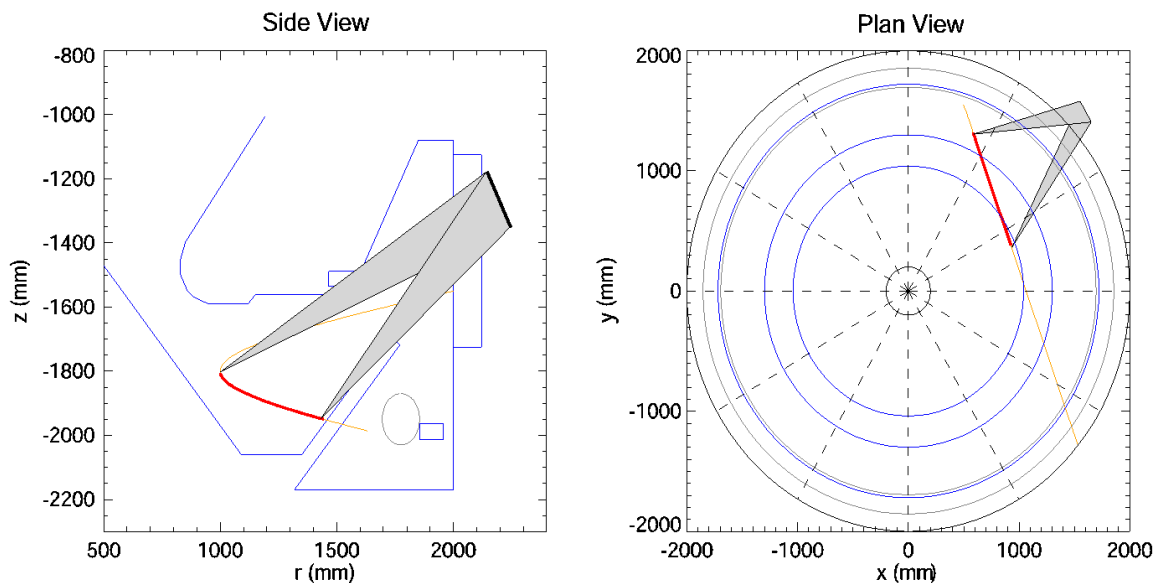


Figure 3. Vignetting simulation showing a side and plan view of the system highlighting the viewing geometry and vignetting concerns at the two extremes of the view region along the laser line.

minimized for the region near the divertor tile at the cost of larger vignetting losses near a radius of 1000 mm. Regions with transmission $< 80\%$ will not be used for TS measurements. Figure 4 shows the calculated losses due to vignetting for this optimized design.

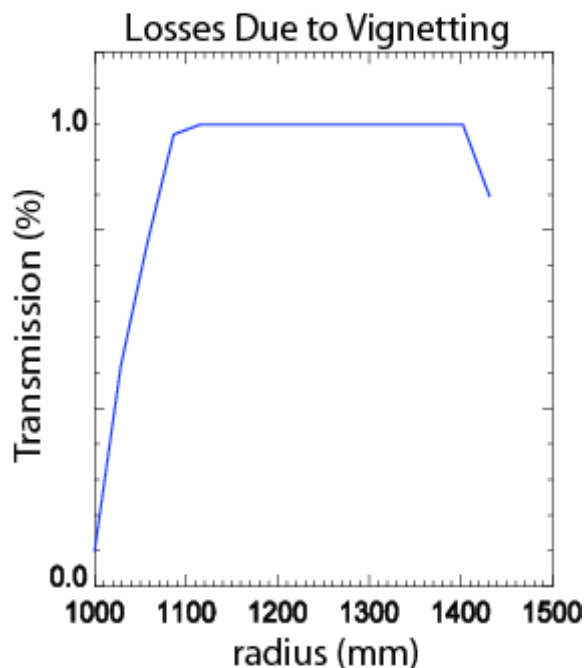


Figure 4. The losses calculated due to vignetting for the designed MAST-U divertor TS system as a function of radius.

3 Radial resolution

Calculations of the expected radial resolution for the MAST-U divertor TS system provided some insight into the diagnostics design. The calculation of the radial resolution was initially set up with the laser within the view region being divided into 100 view segments each with a 10 millimeter scattering length. After the method was confirmed for the fixed laser width (dL) and view width (dV) case, it was expanded to include changes in the laser size and view width as functions of the view location. The calculation of the radial resolution for the system (dr) was performed as an upper bound or worst case scenario given by the maximum radial displacement between the boundary polygon vertices lying on the intersection of the laser and view region boundaries for each collection segment. This calculation process is clarified in figure 5.

The result of this radial resolution calculation is presented in figure 6, which plots the radial resolution (dr) for all 100 view segments. From these results it is clear that the radial resolution is larger than the width of the laser line over the entire collection region. Although this difference between the laser width and the radial resolution does lead to an increased collection of background plasma light it is necessary to retain the fiber geometry to maintain device flexibility. Initially the diagnostic will contain 10 spectrometers & fiber bundles able to be positioned to measure signals at any of the 100 defined spatial locations. Positions near the divertor tile will have a laser width > 5 mm and require the fiber's full 7 mm height perpendicular to the laser line to accommodate the large laser width. To reduce the background level, apertures could be installed to increase the signal-to-noise ratio. This worst case scenario approximation for the radial resolution highlights that over the entire view region the radial resolution is still operating within the required

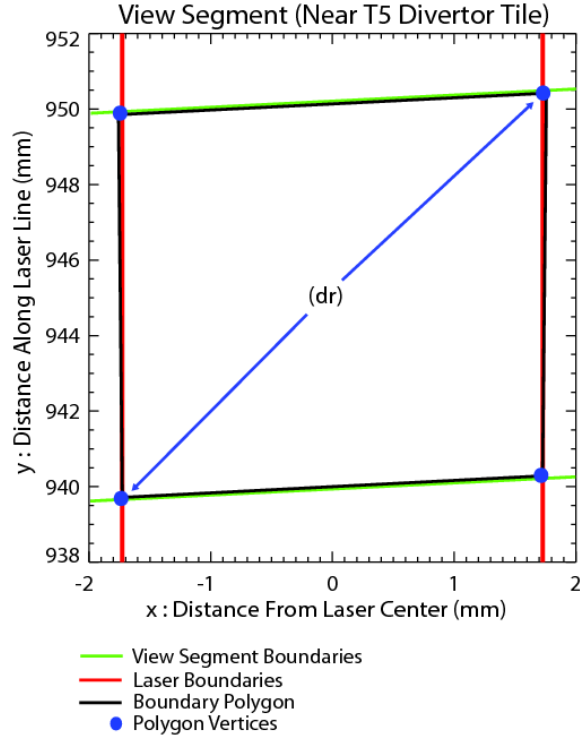


Figure 5. The radial resolution (dr) calculation process defined as the maximum displacement of the boundary polygon vertices formed via the boundaries of the laser line and view segment defined by the collection optics.

specifications (on the order of 1 cm) [3]. These results coupled with measurements of the spatial variation of a detached inner divertor leg on MAST suggest that the proposed divertor TS diagnostic should be able to resolve the evolution of the detachment front in the MAST-U super-X divertor without issue.

4 Expected fractional T_e error

In the SXD high background levels and low plasma densities may limit the accuracy of T_e measurements, even with low T_e values allowing for narrow filters to reduce background levels. To understand what should be expected in terms of the quality of T_e measurements performed by this diagnostic, a first order approach was to model the fractional T_e error over the expected measurable temperature range. The expression for the fractional T_e error is defined as

$$\% T_e \text{ error} = \frac{\sigma_{T_e}}{T_e}$$

The calculation was done over the entire T_e range expected for the MAST-U super-X divertor, assuming a Poisson error, a constant $n_e = 5.0 \times 10^{18} \text{ m}^{-3}$, and assuming the current MAST core TS spectrometer layout [5].

With the MAST-U divertor TS system designed to accommodate up to four of the YAG lasers from the current core TS diagnostic [5], there is the ability to fire two lasers simultaneously. The

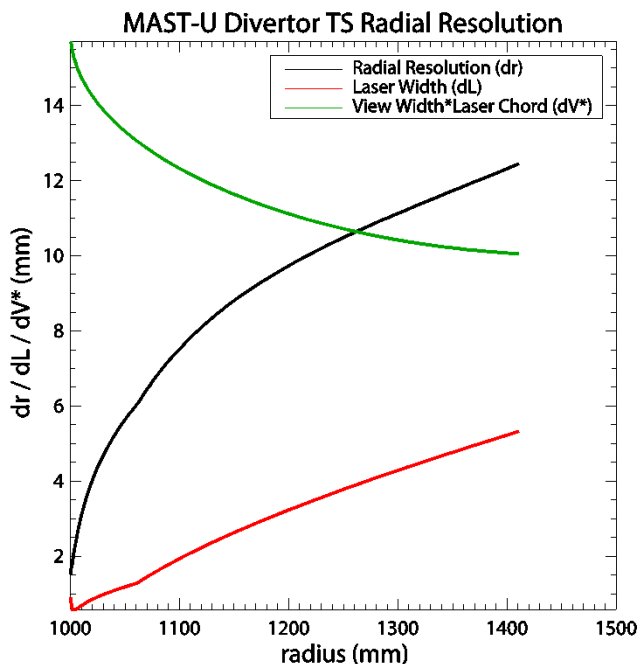


Figure 6. The calculated radial resolution (dr), the laser width (dL), and the observed view width (dV^*) as a function of the radius in millimeters.

injection of two lasers doubles the number of photons available for Thomson scattering, reducing the fractional error of measurements. Using such a technique it is possible to obtain quality T_e measurements in discharges with low divertor plasma density or high background levels that would otherwise not be possible with just 1 J of injected laser energy.

For an initial estimate of the fractional error of the divertor TS diagnostic, calculations were performed using a background solely consisting of an elevated level of bremsstrahlung radiation. The background level within the divertor is expected to have a contribution from line radiation; this and other radiation sources are approximated by the additional radiation above the bremsstrahlung level.

The impact of doubling the injected laser energy is substantial at the low density range that the diagnostic will operate in, reducing the fractional error by approximately 30% over the measureable temperature range, shown in figure 7. The tradeoff of implementing this concept is that it comes with a reduction in the repetition rate of the diagnostic.

5 Laser imaging onto fiber bundle

The fiber packing used in the system as well as how the laser was imaged onto the fiber end for various positions along the laser line have been examined. A transmission function for different packing fractions was developed for two collection cell designs with a different F/#, which are highlighted in table 1. The fiber options investigated in this section are based on the current design found in the MAST core TS system, with 130 fibers in Hexagonal Close Packing, covering a 3 mm diameter fiber end, imaging from F/6 to F/1.75. The designs investigated were an F/6.5 system which used the same fiber packing as the MAST core TS and an F/7.5 system that used

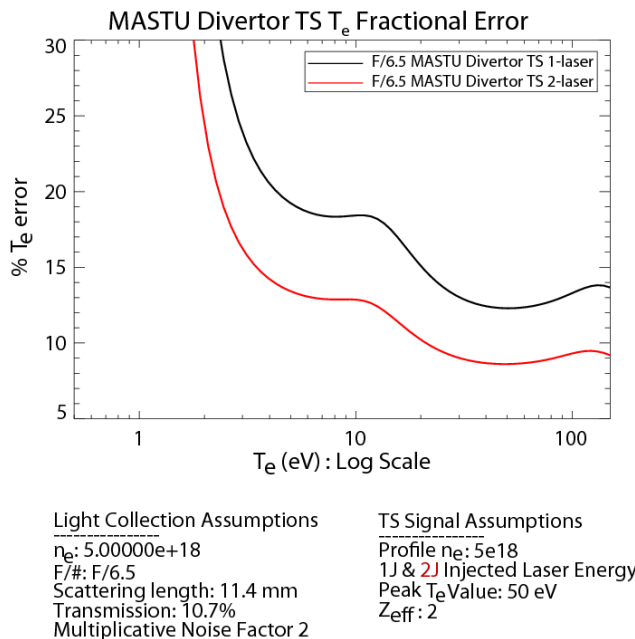


Figure 7. Fractional error calculation for the MAST-U Divertor TS diagnostics with one or two lasers of injected laser energy over the expected Super-X divertor electron temperature range.

Table 1. Two TS collection lens designs with their F/#’s, lens diameters, and dimensions of the fiber backplane used in the investigation of laser imaging onto the fiber bundle.

F/#	Lens Diameter	Fiber Backplane Dimensions
F/6.5	185 mm	3.11 mm \times 2.02 mm
F/7.5	160 mm	3.92 mm \times 1.60 mm

the slightly modified scheme due to the required fiber dimensions. The previously mentioned fiber transmission functions give the percent of rays collected by the fibers with respect to the position on the fiber backplane for both F/# designs. This transmission function was obtained by imaging a fine uniformly spaced grid of “incident rays” covering the entire fiber backplane.

To perform a quantitative analysis of the effect that the laser width, view position, and misalignment has on the intensity of collected light, a ray tracing calculation was performed. This was accomplished using the optical design software, ZEMAX. Inside ZEMAX, three measurement positions along the laser line within the viewing region of the diagnostic were investigated; the position closest to the center column at the start of the viewing region, the position near the divertor T5 tile at the end of the viewing region, and the central position of the laser line within the viewing region of the diagnostic. Over these positions, the laser width varies from 0.9 mm at the position near the center column, to 2.2 mm at the central position, and finally to a maximum of 5.2 mm at the position close to the divertor T5 tile. At each of these three locations, rays were traced from a square source with dimensions corresponding to the associated laser width onto the fiber backplane. At the fiber backplane the image of the laser is examined by plotting the relative illumination scanned along the y-axis along with the generated fiber function. Although results

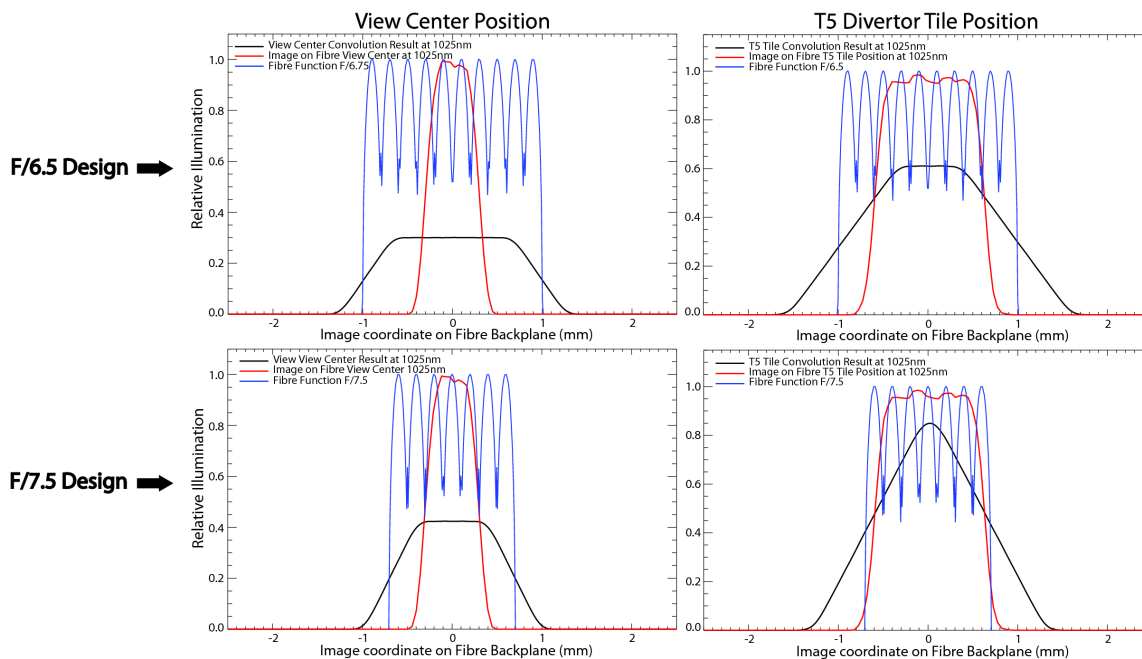


Figure 8. Convolution of the view center position and T5 divertor tile position illumination Y-scan with the corresponding fiber function for the F/6.5 and F/7.5 collection cell system.

presented here just show one wavelength, calculations were performed at five wavelengths in total, spanning 900 nm to 1150 nm.

From the results of the intensity distribution of the laser image onto the fiber backplane it was possible to model the effects of misalignment of the laser image. The method used to examine this effect was to take the results from the illumination Y-scan and perform a convolution of this illumination profile with the calculated fiber packing function for both the F/6.5 and F/7.5 collection optics.

From the results presented in figure 8, the current F/6.5 collection cell design can handle a misalignment of the laser line up to the maximum expected value of nearly 2 mm within the plasma (0.5 mm at the fiber backplane) at all view positions without a sizeable loss in collected TS signal. However, the F/7.5 collection cell design is not as able to accommodate such a misalignment, especially at regions close to the divertor tile where the laser width is large (~ 5 mm). In the F/7.5 case at the T5 divertor tile position, at 0.5 mm misalignment at the fiber backplane only about 60% of the original signal is collected by the fiber bundle. Such a loss of signal near the divertor tile is not acceptable as it is a region of high interest and background levels

6 Depth of field for a multi-laser system

The system was modeled looking at the extreme cases for a four laser system. Using the ZEMAX optical design software, a 185 mm collection lens design collecting at F/6.5 was modified to look at the impact a shift of the depth of field has on the laser image on the fiber. This displacement is the maximum expected shift due to the separation of a four laser system at a position near the divertor tile. It was then applied as the extreme case for the three modeled positions spanning the entire

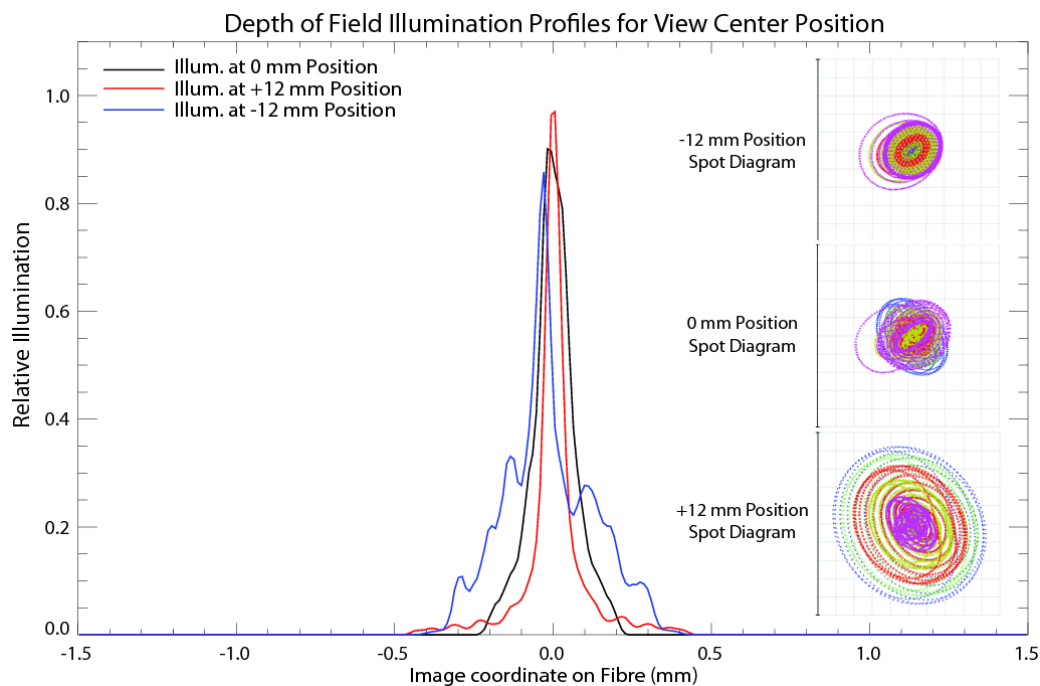


Figure 9. Illumination Y-Scan and spot diagrams of view center position point sources on the fiber backplane for three locations within the depth of field at 1025 nm.

view region of the laser line. To observe the effect a ray tracing analysis was performed for point sources displaced by 0 mm and ± 12 mm within the depth of field for each of the three examined positions.

Change in the depth of field effectively causes a smearing out of the distribution of photons that is put onto the fiber plus some distortion to the spot distribution. The reason the central position is less affected by changes in the depth of field is that altering the depth has no effect on the angle of incidence into the collection optics, as it is positioned on the optical axis. For positions off the optical axis, a change in depth caused by the laser separation alters the collected light's angle of incidence on the collection lens. This causes a more substantial change in the orientation of the imaged photons. To highlight the impact of source displacements within the depth of field figures 9 and 10 show the illumination scan and spot diagram results for the view center and divertor T5 tile positions respectively.

From the results shown in figure 9 and 10, it was concluded that the broadening of the laser image onto the fiber backplane due to depth of field is tolerable. The fiber height perpendicular to the laser propagation is 7 mm and even at the T5 tile position with the laser width being ~ 5.2 mm plus the additional ~ 0.5 mm broadening from the effects of depth is still within the bounds of the 7 mm fiber height. For the 4-laser MAST-U divertor TS system presented, the effects from depth of field were found to be negligible.

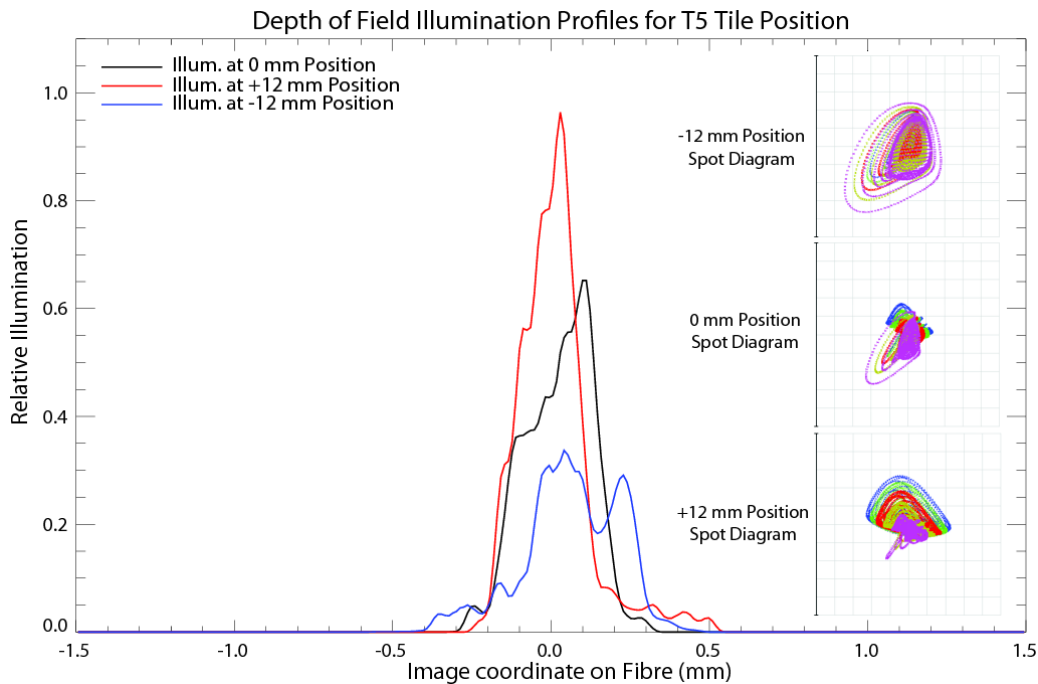


Figure 10. Illumination Y-Scan and spot diagrams of T5 divertor tile position point sources on the fiber backplane for the three locations within the depth of field at 1025 nm.

7 Conclusions

This paper has described an outline of the design and viewing geometry for divertor Thomson scattering as it is to be implemented on MAST-U. The collection cell selected was an F/6.5, 185 mm diameter lens system which focuses on minimizing the vignetting close to divertor tile through the tilt and positioning of this collection cell within the available port. In order to understand the expected resolution of the system, a calculation of radial resolution was performed. This calculation showed that the diagnostic should have the capability to resolve features of interest within/along the super-X divertor, while retaining flexibility in position of measurements.

Performing TS measurements within an extended divertor geometry is expected to have high background level as well as regions of low electron densities that result in a higher fractional error of the diagnostic. The expected fractional error was calculated at a low density of $n_e = 5.0 \times 10^{18} \text{ m}^{-3}$ and a background level above the bremsstrahlung level. This gave an approximation of the fractional error with the impurity concentrations unknown. Finally, the laser width and depth of field effects on the laser image onto the fiber backplane were investigated. The current F/6.5 collection cell design can accommodate the maximum expected misalignment of the laser line of nearly 2 mm within the plasma (0.5 mm at the fiber backplane) and the additional ~ 0.5 mm broadening from the depth of field for all plasma positions.

Acknowledgments

This work was supported by EURATOM and carried out within the framework of the European Fusion Development Agreement. Additionally, this work was partly funded by the RCUK Energy Programme under Grant EP/I501045, by the ITER-NL Programme and by the European Communities under the Contracts of Association between EURATOM, CCFE, and FOM, respectively. The views and opinions expressed herein do not necessarily reflect those of the European Commission.

References

- [1] D.D. Ryutov et al., *The magnetic field structure of a snowflake divertor*, *Phys. Plasmas* **15** (2008) 092501.
- [2] P.M. Valanju et al., *Super-X divertors and high power density fusion devices*, *Phys. Plasmas* **16** (2009) 056110.
- [3] E. Havlíčková et al., *Benchmarking of a 1D scrape-off layer code SOLFID with SOLPS and its use in modelling long-legged divertors*, *Plasma Phys. Control. Fusion* **55** (2013) 065004.
- [4] G. Fishpool et al., *MAST-upgrade divertor facility and assessing performance of long-legged divertors*, *J. Nucl. Mater.* **438** (2013) S356.
- [5] R. Scannell et al., *Design of a new Nd:YAG Thomson scattering system for MAST*, *Rev. Sci. Instrum.* **79** (2008) 10E730.
- [6] E. Havlíčková et al., *Numerical studies of effects associated with the Super-X divertor on target parameters in MAST-U*, *J. Nucl. Mater.* **438** (2013) S545.